Atmospheric Environment 237 (2020) 117704

Contents lists available at ScienceDirect

Atmospheric Environment

journal homepage: http://www.elsevier.com/locate/atmosenv

Chemical composition and seasonal variations of $PM_{2.5}$ in an urban environment in Kunming, SW China: Importance of prevailing westerlies in cold season

Yunhong Zhou [a,b], Huayun Xiao [a,*], Hui Guan [a,**], Nengjian Zheng [c], Zhongyi Zhang [c], Jing Tian [a,b], Linglu Qu [d], Jingjing Zhao [a,b], Hongwei Xiao [c]

[a] State Key Laboratory of Environmental Geochemistry, Institute of Geochemistry, Chinese Academy of Sciences, Guiyang, 550081, China
[b] University of Chinese Academy of Sciences, Beijing, 100049, China
[c] Key Laboratory of the Causes and Control of Atmospheric Pollution, East China University of Technology, Nanchang, 330000, China
[d] State Key Laboratory of Environmental Criteria and Risk Assessment, Chinese Research Academy of Environmental Sciences, Beijing, 100012, China

HIGHLIGHTS

- $PM_{2.5}$ and its major water-soluble inorganic ions were characterized in Kunming.
- Five source factors were identified for $PM_{2.5}$ by PMF.
- Coal combustion played a leading role in the source contribution of $PM_{2.5}$ in winter.
- In winter, air pollutants from India could be brought to Kunming by prevailing westerlies.
- In spring, the sources of $PM_{2.5}$ were mainly affected by biomass burning from South Asia and Southeast Asia.

GRAPHICAL ABSTRACT

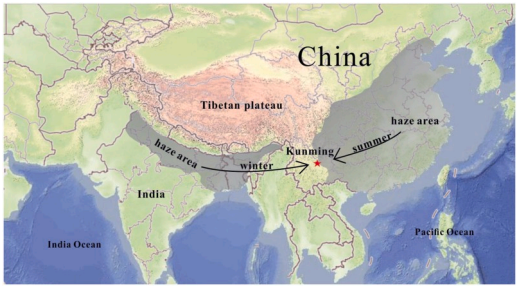

ARTICLE INFO

Keywords:
$PM_{2.5}$
Water-soluble inorganic ions
Positive matrix factorization
Back trajectory
Prevailing westerlies

ABSTRACT

Kunming, a Chinese southwestern tourist city which has not large local pollution sources, has found to have an increasing tendency of haze pollution in recent years. But the pollution sources are unclear. In order to identify them, daily $PM_{2.5}$ samples (n = 346) were collected from September 2017 to August 2018 in the urban area. And the major water-soluble inorganic ions (WSIIs) were determined to better understand the chemical characteristics, source categories and potential region of sources. Our study showed that the mass concentration of $PM_{2.5}$ in Kunming ranged from 7.61 to 91.83 μg m^{-3}, with an annual average value of 33.59 ± 15.71 μg m^{-3}. Positive matrix factorization (PMF) model identified five factors including secondary aerosol (the contributions of 36.3%), coal combustion (26.0%), biomass burning (19.2%), dust (12.5%) and sea salt (6.0%). And coal combustion played a leading role in the source contribution of $PM_{2.5}$ in winter while biomass combustion was dominant in spring. Being located between two severe haze zones in the world, northern-central China and north of South Asia, and affected by India monsoon and East Asia monsoon in summer and prevailing westerlies in winter, we found that air masses from South Asia (especially India) contained pollutants could be brought to

* Corresponding author.
** Corresponding author.
E-mail addresses: xiaohuayun@vip.gyig.ac.cn (H. Xiao), guanhui@mail.gyig.ac.cn (H. Guan).

https://doi.org/10.1016/j.atmosenv.2020.117704
Received 26 August 2019; Received in revised form 3 April 2020; Accepted 9 June 2020
Available online 12 June 2020

Kunming by prevailing westerlies in winter. In spring, however, the sources of $PM_{2.5}$ in Kunming were mainly affected by biomass burning from South Asia and Southeast Asia when prevailing westerlies gradually weakened.

1. Introduction

World Health Organization has released a report that nine out of ten people are breathing polluted air around the world, seven million people die from indoor and outdoor air pollution every year (WHO, 2018), with 24% of them from stroke deaths, 29% from lung cancer, 25% from heart disease and 43% from other lung diseases (WHO, 2018). Atmospheric $PM_{2.5}$ (particulate matters with aerodynamic equivalent diameter < 2.5 μm) is a crucial air pollutant which can exert adverse effects on human health, climate and visibility (Chin et al., 2009; Chow et al., 2006; Pope et al., 2009; Zhang et al., 2010). Numerous researches have indicated that massive inhalation of particles is more likely to increase the morbidity of acute respiratory infections, lung cancer and cardiovascular diseases (Dockery et al., 1993; Ou et al., 2019; Pope et al., 2009, 2015; Ramgolam et al., 2009). Aerosol can be derived from multiple sources. Primary sources such as soil emission, sea salt, coal combustion, vehicle exhaust, biomass combustion are derived from natural sources and anthropogenic sources (Chin et al., 2009). Secondary aerosols are formed during the transformation from gaseous precursors (NH_3, SO_2, NO_X and VOC) to particles (Chin et al., 2009). Aerosols generated from different sources and processes have different chemical and isotopic compositions. Besides, water-soluble inorganic ions (WSIIs) of $PM_{2.5}$ are so important, which affect the acidity and nucleation ability of aerosols, and can change their size and lifetime owing to their hygroscopic properties (Tang, 1996). Chemical characteristics and source apportionments of $PM_{2.5}$ have been reported in plenty of studies (Liu et al., 2016a; Souza et al., 2014; Wang et al., 2016b; Xiao et al., 2017).

The heating activities in winter exert direct impact on haze pollution in northern China, and the winter monsoon further widened the haze area. A large number of researches have been carried out on areas with severe fog and haze in the North China Plain, Guanzhong Plain, Sichuan basin, Yangtze River Delta and Pearl River Delta (Tan et al., 2009; Tao et al., 2013; Wang et al., 2015, 2016b; Yao et al., 2002; Ye et al., 2003). But there is still a lack of systematic knowledge of chemical compositions and source apportionments of $PM_{2.5}$ in Yunnan-Guizhou Plateau. Known as "spring city", the temperature in Kunming is relatively uniform all the year round. Shi et al. (2016) studied the characteristic of chemical components of WSIIs and element carbon (OC and EC) in $PM_{2.5}$ based on 28 filter samples and reported that the average concentration of $PM_{2.5}$ in Kunming was highest in spring (105.88 ± 48.03 μg m^{-3}), followed by winter (92.66 ± 51.56 μg m^{-3}), autumn (74.73 ± 41.39 μg m^{-3}) and summer (72.19 ± 30.26 μg m^{-3}). Qiao et al. (2018) conducted a research based on CMAQ model to assess the source contributions to $PM_{2.5}$ and found that industrial and residential activities were predicted to be the largest contributor in 25 Chinese cities including Kunming (provincial capitals and municipalities) for the year of 2013. In addition, there were some investigations of $PM_{2.5}$ concentrations and chemical species in most important cities in China with the goals of understanding spatial and temporal trends and quantifying the regional component of PM pollution, in which Kunming showed relatively less polluted characteristic than those cities distributed in the north of China (Liu et al., 2018; Xu et al., 2017; Yuan et al., 2018). In general, there are lacking of high time resolution research on the compositions of $PM_{2.5}$ filter samples in Kunming. However, this city has found to have an increasing tendency of haze pollution in recent years. Located between the world's two severe haze zones, northern-central China and north of South Asia (Air Pollution in Asia: Real-time Air Quality Index Visual Map, http://aqicn.org/map/), what caused the haze pollution in Kunming was worth further exploring.

In this study, the major water-soluble inorganic compositions of $PM_{2.5}$ were analyzed from September 2017 to August 2018 to examine the pollution level and characterize the seasonal variations of $PM_{2.5}$ in Kunming. Positive matrix factorization (PMF) model were used to identify the source categories and their contributions. The routes of air masses transported to the study site were traced by back trajectory. This has substantial implications for the development of efficient remediation policies to better improve the air quality.

2. Method

2.1. Sampling site and collection

Kunming is located in the south of 30°N, where solar radiation can be relatively evenly received throughout the year. Affected by the Indian monsoon and East Asia monsoon in summer (Fig. 1), the rainy season in Kunming is formed from May to October. In addition, with an average altitude of 1892 m in Yunnan-Guizhou Plateau, the cool climate can be kept in Kunming because temperature decreases progressively with altitude. In winter, warm and dry air from the Indian Peninsula can be brought by prevailing westerlies to Kunming. Mountain Liangwang and Mountain Wumeng, respectively located in the north and east of Kunming, can block the cold air from north China (Fig. 1).

Aerosol samples of $PM_{2.5}$ were collected using quartz filters (8×10 inch, Tissuquartz™ Filters, 2500 QAT-UP, Pallflex, Washington, USA) and KC-1000 sampler (Laoshan Institute for Electronic Equipment, Qingdao, China) at a high flow rate (1.05 ± 0.03 m^3 min^{-1}). The sampler was installed on the top of teaching building in Kunming University of Science and Teaching (102.70°N, 25.06°E). The study site is located in the center area of Kunming and close to the north of the first ring road. The sampling time started at 9:00 to 10:00 a.m. and lasted for 23.5 h. Daily samples were collected and immediately storaged in the refrigerator at −20 °C until chemical analysis. A total of 346 aerosol samples were obtained during this sampling campaign (from September 1, 2017 to August 31, 2018).

2.2. Chemical analyses

Sample pretreatment: All sample filters were weighed before and after sampling, and were analyzed gravimetrically for mass concentrations. One-eighth filters of daily $PM_{2.5}$ samples were used for chemical analyses. WSIIs were extracted in 50 mL deionized water (Millipore, 18.2 MΩ) using an ultrasonic bath for 30 min at room temperature. After ultrasound, the supernatant was centrifuged at 4200 r/min for 10 min and filtered with 0.22 μm pinhole filter. The obtained total water extract was rinsed twice with 5 ml ultrapure water. The extract and rinse were put into a pre-cleaned 50 ml tube together and stored in a refrigerator at −20 °C until chemical analyses.

The major water-soluble inorganic species (cation: Na^+, NH_4^+, K^+, Mg^{2+}, Ca^{2+}, and anion: F^-, Cl^-, NO_3^-, SO_4^{2-}) in the extract were analyzed using the ion chromatograph (model ICS-1100 and ICS-900 for anion and cation), which equipped with a conductivity detector (ASRS-ULTRA), suppressor (ASRS-300 for the ICS-1100 and CSRS-300 for the ICS-900), and separator columns (AS11-HC for anions and CS12A for cations) and guard columns (AG11-HC for anions and CG12A for cations) were used in the analyses. The precision for all ionic species was better than 5%. And the detection limits of this method were Cl^- at 0.0051 ppb, NO_3^- at 0.0216 ppb, SO_4^{2-} at 0.0115 ppb, and Na^+ at 0.001 ppb, NH_4^+ at 1.21 ppb, K^+ at 1.77 ppb, Mg^{2+} at 2.47 ppb and Ca^{2+} at 0.09 ppb.

2.3. Meteorological data

Meteorological data during the sampling period (September 1, 2017–August 31, 2018) in Kunming were obtained from National Meteorological Information Center (http://data.cma.cn/data/, Fig. 2), including wind speed, temperature, relative humidity, rainfall. Atmospheric SO_2 and NO_2 data were downed from National Urban Air Quality Real-Time Publishing Platform (http://106.37.208.233:20035/). The sampling period was divided into autumn, winter, spring, summer by every three months. Meteorological condition plays a vital role in determining both the transport and the distribution of air pollutants. The average temperature of each season was 16.0 °C, 9.5 °C, 16.9 °C and 20.2 °C, respectively, with annual average temperature is 15.6 °C (Fig. 2d). Annual average relative humidity was 71.5% (Fig. 2c). It's windy and dry in March and April (Fig. 2a and c). Kunming is well known for its intense solar radiation and holds two distinct dry-wet seasons, the wet season (May–October) which accounts for 85% of the annual rainfall (Qin et al., 2010) (Fig. 2b).

2.4. PMF model

PMF (v5.0) is a multivariate statistical model for identifying source categories and quantifying the contributions of different sources to a group of samples. And it is widely used in source apportionment of atmospheric particulate matte (Liu et al., 2017; Sharma et al., 2016). A specified data matrix is decomposed into two sub-matrices by PMF: factor contribution matrix (*g*) and factor profile matrix (*f*) (Paatero, 1997; Paatero and Tapper, 1994). The data set can be regarded as a data matrix *x* of *i* by *j* demention.

$$x_{i\cdot j} = \sum_{k=1}^{p} g_{i\cdot k} f_{k\cdot j} + e_{i\cdot j}$$

$x_{i\cdot j}$ represents the concentration of the jth species in the ith sample, $g_{i\cdot k}$ is related with the kth contribution factor measured in the ith sample, $f_{k\cdot j}$ means the jth species fraction from the kth source, $e_{i\cdot j}$ is the residual of the jth species in the ith sample, and p is the total number of independent sources categories.

The object function Q minimizes based upon these equation as follows:

$$Q = \sum_{i=1}^{n} \sum_{j=1}^{m} \left[\frac{x_{i\cdot j} - \sum_{k=1}^{p} g_{i\cdot k} f_{k\cdot j}}{u_{i\cdot j}}\right]^2$$

Where $u_{i\cdot j}$ is the uncertainty.

If the concentration is less than or equal to the MDL (method detection limit) provided, the uncertainty (*Unc*) is calculated using a fixed fraction of the MDL, which is calculated as $Unc = 5/6 * MDL$. If the concentration is greater than the provided MDL, and the calculation is based on a user provided fraction of the concentration and MDL, which is defined as $Unc = \sqrt{(ErrorFraction * concentration)^2 + (0.5 * MDL)^2}$ (Polissar et al., 1998).

In this study, PMF 5.0 (US EPA 2014) model was applied for source apportionments of major water-soluble inorganic ions (F^-, Cl^-, NO_3^-, SO_4^{2-}, Na^+, $NH4^+$, K^+, Mg^{2+} and Ca^{2+}).

2.5. Backward trajectories analysis

72-h air mass back trajectories were computed for the whole sampling days (from September 1, 2017 to August 31, 2018) using the NOAA's program of TrajStat software to analyze the routes of air masses transported to the study site (Almeida et al., 2015; Liu et al., 2016a; Zhang et al., 2014). Meteorological of NCEP GDAS data were downloaded from the National Oceanic and Atmospheric Administration Laboratory (NOAA ARL) on the website (ftp://arlftp.arlhq.noaa.gov/archives). The back trajectories were calculated for all sampling days and started at 16:00 UTC (Beijing time is 00:00). The arrival level of the air masses were set at 1000m above the study site. In this study, trajectories were classified optimally using the clustering method for different seasons. And four or five clustering trajectories were obtained each season.

3. Result and discussion

3.1. $PM_{2.5}$ and chemical species

3.1.1. Characteristics of ambient $PM_{2.5}$

The mass concentrations of $PM_{2.5}$ in Kunming ranged from 7.61 to 91.83 μg m^{-3}, with an annual average concentration of 33.59 ± 15.71 μg m^{-3}, which is below the Chinese National Ambient Air Quality Standards (NAAS, 35 μg m^{-3}). This is similar to a previous report (30.9 ± 17.5 μg/m^3) in Kunming from 2013.4 to 2014.3 (data from China National Environmental Monitoring Center) (Yin et al., 2016) and within the range of 22–42 μg/m^3 from 2014 MODIS satellite remote sensing aerosol data of $PM_{2.5}$ in this plateau city (Yuan et al., 2018). In addition, the annual average concentration of $PM_{2.5}$ in Kunming was lower than those in other major cities of China like Beijing (154.3 ± 145.7 μg m^{-3}) (Wang et al., 2005), Shanghai (63.4 μg m^{-3}) (Ye et al., 2003), Tianjin (141.47 μg m^{-3}), Shijiazhuang (191.19 μg m^{-3}), and Chengdu (92.41 μg m^{-3}) (Zhao et al., 2013), while it was higher than those at the rural areas, such as southwestern rural Nevada, USA (5.1 μg

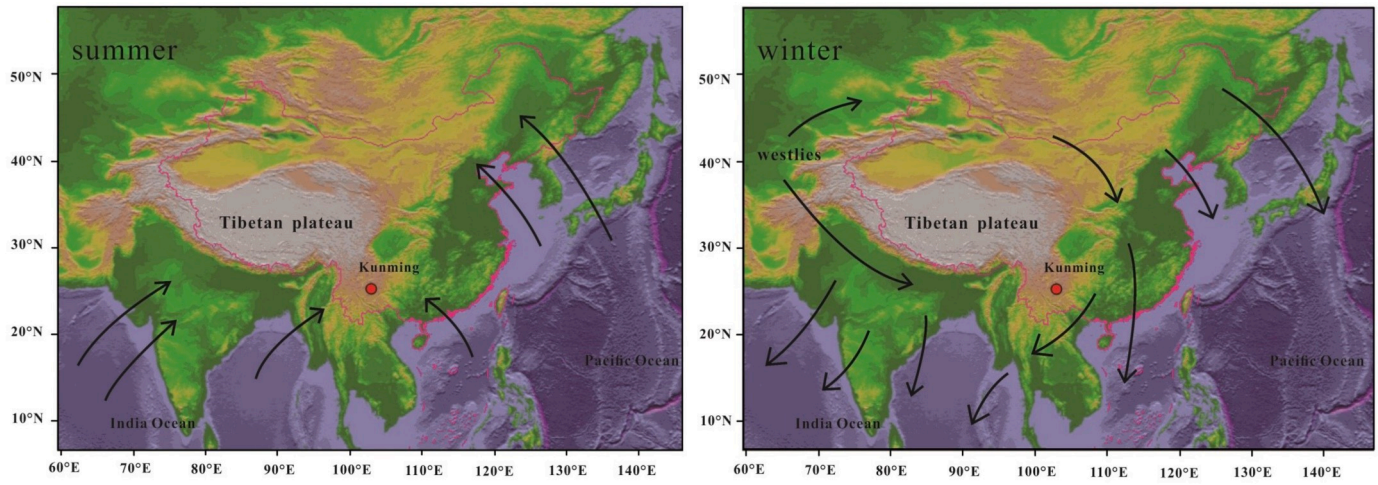

Fig. 1. Map of wind direction in Eastern Asia including winter monsoon and prevailing westerlies during winter and summer monsoon during summer.

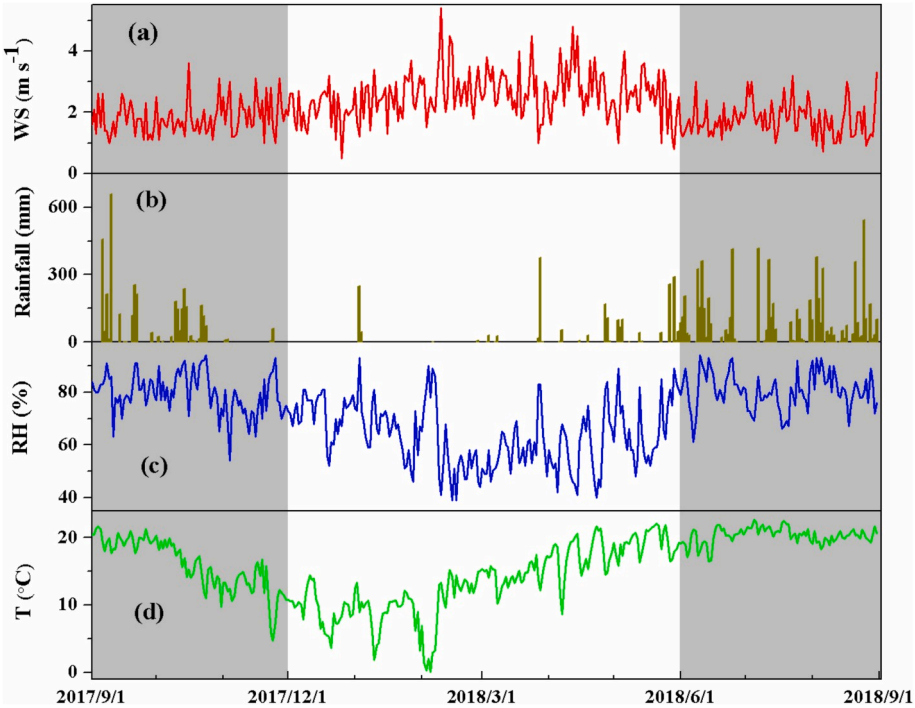

Fig. 2. Meteorological parameters including Temperature (°C), relative humidity (%), rainfall (mm), wind speed (m s^{-1}) in Kunming during sampling period. (the shaded areas represent cold season, unshaded areas represent warm season).

m^{-3}) (Engelbrecht et al., 2015), Edinburgh in UK (8.5 μg m^{-3}) (Heal et al., 2005), and a rural site in Crete (18.2 μg m^{-3}) (Gerasopoulos et al., 2007), reveling a less $PM_{2.5}$ pollution in Kunming urban atmosphere.

Monthly average mass concentrations of $PM_{2.5}$ were showed in Fig. 3a, which were higher in cold season than those in warm season. This seasonal variations is consistent with previous studies in Kunming (Liu et al., 2018; Shi et al., 2016). And the parallel seasonal variations were reported in other study areas (Liu et al., 2017; Wang et al., 2015; Xiao et al., 2017; Zhang et al., 2014). This was ascribed to a combination of factors including atmospheric condition (including WS, Rainfall, T, RH and solar radiation etc.) and sources. Same as the previous study (Shi et al., 2016), dust from bared soil induced by higher WS (Fig. 2a) caused the high concentrations of $PM_{2.5}$ in spring (Table 2); in addition, temperature inversion layer could be induced to both scatter and absorb solar radiation, which suppressed dispersion of pollutants and led to further accumulation of particles (Li et al., 2017b). In warm season, the concentrations of particulate matters could be rapidly reduced due to frequent precipitations (Fig. 2b), which is an effective way to scavenge particles from the atmosphere. And stronger airflow was benefit for the diffusion of pollutants.

3.1.2. *Characteristics of chemical species in $PM_{2.5}$*

The major WSIIs accounted for 46–48% of $PM_{2.5}$ during different seasons, with an annual average value of 15.51 μg m^{-3}. As shown in Figs. 3b and 4, SO_4^{2-} had the highest concentrations from 1.36 to 17.18 μg m^{-3}, with annual average value of 6.82 ± 3.34 μg m^{-3}. The other major WSIIs concentrations in $PM_{2.5}$ samples decreased in the following orders: NH_4^+ (0.058–9.67 μg m^{-3}; average: 2.62 ± 1.55 μg m^{-3}) > NO_3^- (0.53–12.60 μg m^{-3}; average: 2.48 ± 1.84 μg m^{-3}) > Ca^{2+} (0.27–7.04 μg m^{-3}; average: 2.32 ± 1.08 μg m^{-3}) > Cl^- (0.06–3.86 μg m^{-3}; average: 0.49 ± 0.45 μg m^{-3}) > K^+ (0.005–7.86 μg m^{-3}; average: 0.43 ± 0.52 μg m^{-3}) > F^- (0.004–0.91 μg m^{-3}; average: 0.16 ± 0.14 μg m^{-3}) > Mg^{2+}

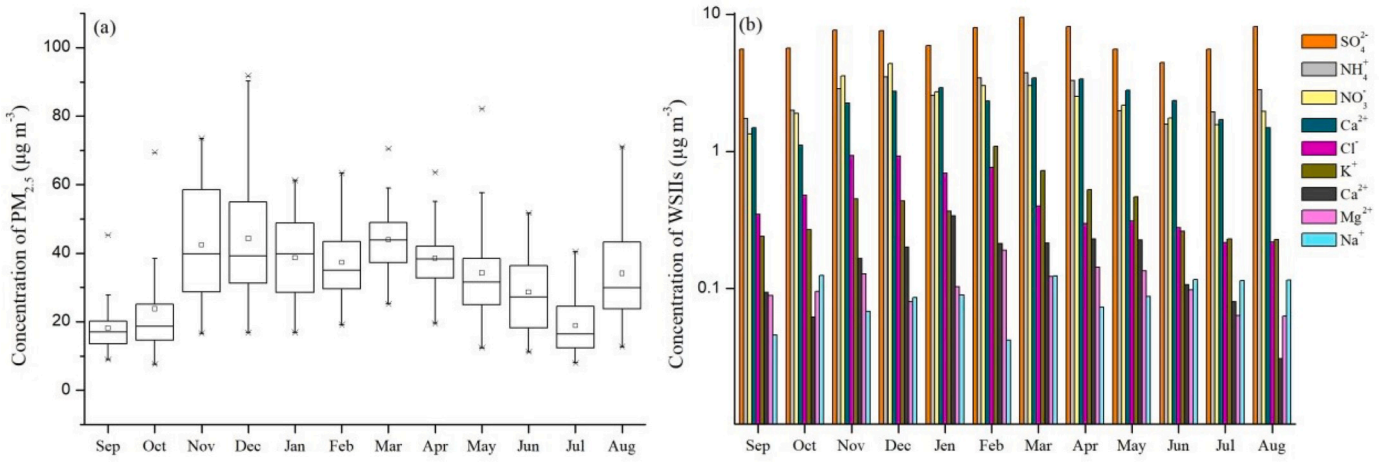

Fig. 3. Variations of monthly average concentrations for (a) $PM_{2.5}$ and (b) water soluble inorganic ions (WSIIs) in Kunming.

Table 1
Correlation coefficients among major water-soluble inorganic ions in aerosol and meteorological parameters.

	$PM_{2.5}$	NO_3^-	SO_4^{2-}	F^-	Cl^-	NH_4^+	Ca^{2+}	K^+	Na^+	Mg^{2+}
$PM_{2.5}$	1	.638[a]	.616[a]	.279[a]	.497[a]	.622[a]	.430[a]	.549[a]	.130*	.267[a]
NO_3^-		1	.739[a]	.042	.453[a]	.791[a]	.403[a]	.429[a]	.025	.133*
SO_4^{2-}			1	.008	.298[a]	.881[a]	.395[a]	.490[a]	.039	.216[a]
F^-				1	.248[a]	.027	.515[a]	.378[a]	.055	.333[a]
Cl^-					1	.298[a]	.167[a]	.293[a]	.127*	.477[a]
NH_4^+						1	.455[a]	.552[a]	.049	.158[a]
Ca^{2+}							1	.615[a]	.115	.365[a]
K^+								1	.211*	.670[a]
Na^+									1	.122*
Mg^{2+}										1

[a] Correlation significant at 0.01 level (two-tailed), * significant at 0.05 level (two-tailed).

Table 2
Water-soluble inorganic ions and mass concentrations of NO_2, SO_2 (mean ± SD, unit: μg m^{-3}), and their relationship (NOR, SOR, NO_3^-/SO_4^{2-}) in Kunming during sampling time.

	autumn	winter	Spring	summer	annual
$PM_{2.5}$	28.16 ± 17.17	40.18 ± 14.69	38.86 ± 12.48	27.11 ± 13.65	33.59 ± 15.71
F^-	0.11 ± 0.01	0.25 ± 0.01	0.22 ± 0.01	0.07 ± 0.01	0.16 ± 0.14
Cl^-	0.59 ± 0.04	0.79 ± 0.04	0.34 ± 0.02	0.24 ± 0.02	0.49 ± 0.45
NO_3^-	2.25 ± 0.17	3.36 ± 0.18	2.56 ± 0.14	1.76 ± 0.14	2.48 ± 1.84
SO_4^{2-}	6.31 ± 0.46	7.19 ± 0.39	7.73 ± 0.43	6.05 ± 0.48	6.82 ± 3.34
K^+	0.32 ± 0.02	0.63 ± 0.03	0.57 ± 0.03	0.24 ± 0.02	0.43 ± 0.52
Na^+	0.08 ± 0.01	0.07 ± 0.00	0.09 ± 0.01	0.12 ± 0.01	0.09 ± 0.08
Ca^{2+}	1.61 ± 0.12	2.66 ± 0.15	3.20 ± 0.18	1.85 ± 0.15	2.32 ± 1.08
Mg^{2+}	0.10 ± 0.01	0.12 ± 0.01	0.13 ± 0.01	0.07 ± 0.01	0.10 ± 0.06
NH_4^+	2.20 ± 0.16	3.17 ± 0.17	3.00 ± 0.17	2.11 ± 0.17	2.62 ± 1.55
SO_2	21.84 ± 15.3	22.01 ± 10.6	15.43 ± 7.14	19.44 ± 16.9	19.68 ± 12.54
SOR	0.25	0.27	0.35	0.27	0.28
NO_2	2.25 ± 1.84	3.36 ± 2.49	2.56 ± 1.18	1.76 ± 1.03	2.5 ± 1.8
NOR	0.06	0.08	0.07	0.05	0.06
NO_3^-/SO_4^{2-}	0.35	0.45	0.34	0.31	0.36

(0.004–1.02 μg m^{-3}; average: 0.10 ± 0.06 μg m^{-3}) > Na^+ (0.001–0.63 μg m^{-3}; average: 0.09 ± 0.08 μg m^{-3}). Except that the concentrations of Na^+ were slightly higher in summer than those in other three seasons, the other major WSIIs showed the same seasonal variation pattern as $PM_{2.5}$, with higher concentrations in the cool season than in the warm season (Table 2).

The three ions SO_4^{2-}, NO_3^- and NH_4^+ accounted for 74.53%–85.96% of the total WSIIs. The pie charts for ion fractions of aerosols for different seasons are shown in Fig. 4. The proportions of sulfate in $PM_{2.5}$ in warm season were much higher than that in cold season while the proportions of nitrate and ammonium increased in winter. It was found that SO_4^{2-} and NO_3^- were well correlated with NH_4^+, with a correlation coefficient of 0.881 between SO_4^{2-} and NH_4^+ and 0.791 between NO_3^- and NH_4^+ (Table 1). NH_4^+ is mainly produced by the neutralization reaction between gaseous NH_3 and acidic sulfate and nitrate particles during gas-particle conversion process. The majority of aerosol pH were simulated as acidic using ISORROPIA-II model. These ions mainly existed in the form of NH_4NO_3, NH_4HSO_4 and $(NH_4)_2SO_4$.

Ca^{2+} showed good correlation with nitrate ($R^2 = 0.403$) and sulfate ($R^2 = 0.395$) (Table 1). Yunnan-Guizhou plateau is well-known as a typical Karst plateau area. Calcium carbonate accounted for considerable proportions of rocks here. This might indicate the existence of $Ca(NO_3)_2$ and $CaSO_4$ in particulate matter. The concentrations and the fractions of Ca^{2+} in spring were much higher than those in other seasons (Table 2 and Fig. 4), which suggested that higher wind speed in spring could be benefit to produce mineral dust.

K^+ is a major component in the sintering plant stack (Almeida et al., 2015). Besides, K^+ has been widely used as an important indicator of biomass burning (Pant and Harrison, 2012). As shown in Table 1, K^+ owned good correlations with SO_4^{2-} ($R^2 = 0.490$) and NO_3^- ($R^2 = 0.429$), but monthly variation of K^+ was not synchronized with SO_4^{2-} and NO_3^- (Fig. 3b), suggesting that K^+ and anions (SO_4^{2-} and NO_3^-) might be dominated by different sources. In addition, monthly variation of K^+ showed that the concentrations of K^+ increased from February to May, and biomass burning in Southeast Asia prevailed at the same season. So we inferred that K^+ was most likely to be derived from biomass burning. And K^+ owned good correlations with all the anions and Ca^{2+}, On one hand, it has been found that biomass burning was a dominant source of SO_4^{2-} and NO_3^- in southern Asia (Lawrence and Lelieveld, 2010). This might explain why K^+ owned good relationship with SO_4^{2-} and NO_3^-. On the other hand, Biomass burning, like straw combustion, could bring out some ions from soil, so this K^+ was significantly correlated with Ca^{2+}, and the correlation coefficient reached 0.615.

Na^+ showed poor correlation with other ions. As for Na^+, it can be originated from sea salt as NaCl, soil and road dust, etc. The seasonal average concentration of Na^+ in summer was slightly higher than those in other three seasons (Table 2) due to summer monsoon. It could be inferred that Na^+ was mainly dominated by sea salt in Kunming. Considering that Kunming is an inland city, the poor correlation between Cl^- and Na^+ might due to the depletion of Cl^- occurred as H_2SO_4 and HNO_3 reacts with sea salt during air masses transport (Yao et al., 2003). The Cl^- in this study was mainly derived from other anthropogenic sources, such as coal combustion. It could be inferred from inconspicuous seasonal variations of Na^+ that it's hard for air masses from coastal areas to be transported to inland Kunming.

3.1.3. NO_3^-/SO_4^{2-}, SOR and NOR

The ratio of NO_3^-/SO_4^{2-} can be used to evaluate the contribution of mobile sources and stationary sources to sulfur and nitrogen in the atmosphere (Cao et al., 2009; Xiao and Liu, 2004). During the sampling period, the mass ratio of NO_3^-/SO_4^{2-} was in the range of 0.12–1.08, with the mean value of 0.36. This ratio in Kunming was comparable to Fuzhou (0.37) (Xu et al., 2012), Hangzhou (0.36) (Cao et al., 2009); and Qingdao (0.35) (Hu et al., 2002), where the densities of the vehicles in those cities were lower than those in Beijing (0.71) (Wang et al., 2005), shanghai (0.64) (Wang et al., 2006), Guangzhou (0.64) (Tan et al., 2009), and the consumption of coal (stationary emission) in Kunming was much lower than that in Guiyang (0.14) (Xiao and Liu, 2004), where the coal combustion caused big problems of environmental pollution. It could be inferred from the mass ratio of NO_3^-/SO_4^{2-} that mobile sources and stationary sources both contributed less to PM $_{2.5}$ in Kunming compared to other cities.

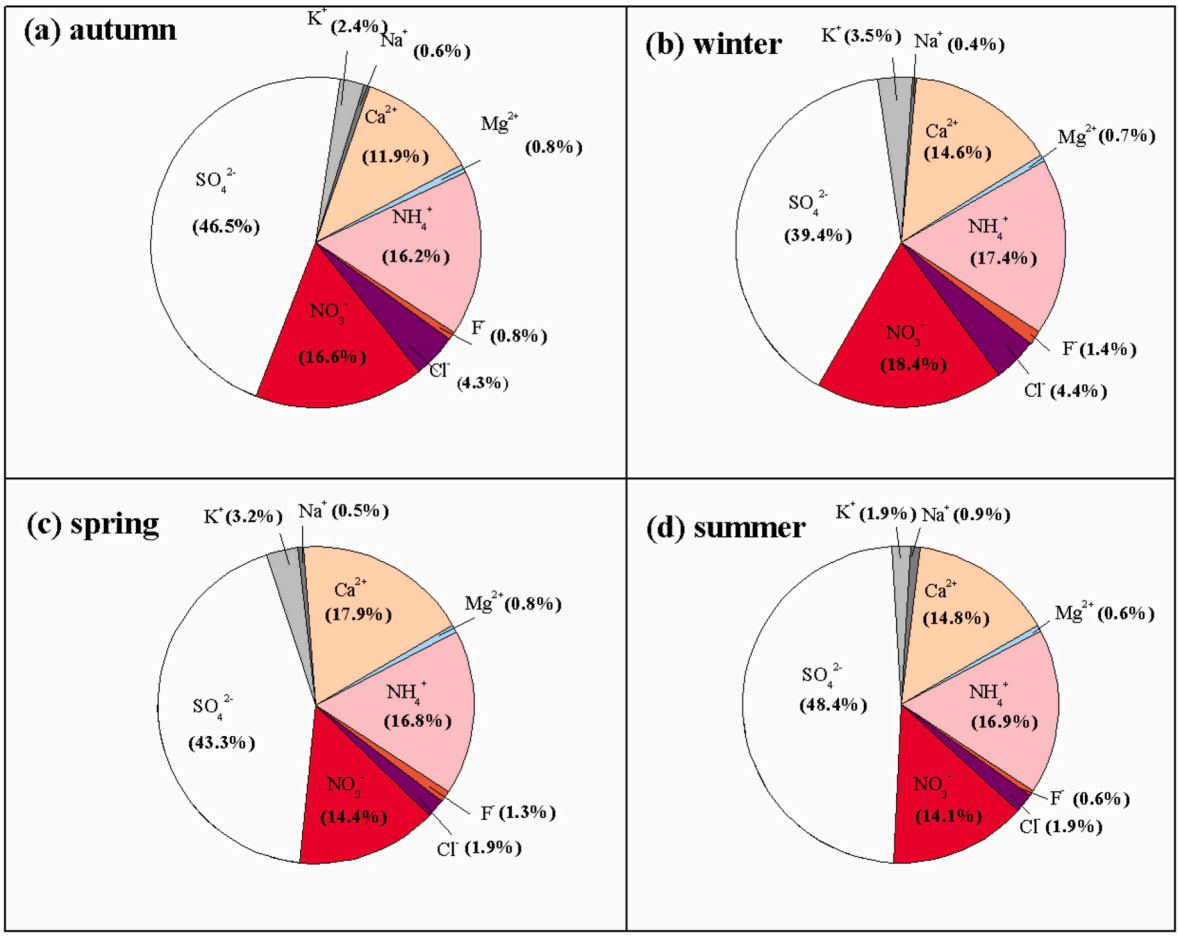

Fig. 4. Pie charts for mean contributions of each component to total mass concentration in (a) autumn, (b) winter, (c) spring and (d) summer, respectively.

Nitrogen oxidation ratio (NOR) and the sulfur oxidation (SOR) were used to evaluate the photochemical oxidation extent of SO_2 and NO_2 (Luo et al., 2019; Ohta and Okita, 1990; Sun et al., 2006). NOR and SOR are defined as the ratio of second species to total N or total S, NOR = $nNO_3^-/(nNO_3^- + nNO_2)$, SOR = $nSO_4^{2-}/(nSO_4^{2-} + nSO_2)$, where n refers to molar concentration. Gas precursors SO_2 and NO_2 showed the same seasonal variation patterns as $PM_{2.5}$ and major ions (Table 2). Ohta and Okita (1990) suggested the existence of photochemical oxidation of SO_2 and NO_2 in the atmosphere when SOR and NOR exceeded 0.10. In this study, SOR was greater than 0.10 in all four seasons (Table 2). In addition, SOR was comparable among summer, autumn and winter, while it was higher in spring. This indicated that photochemical oxidation of SO_2 occurred all year round and was more efficient in spring, which was related to higher solar radiation in spring in Kunming. The sudden increase of SO_4^{2-} in August (Fig. 3b) could be explained as the promotion of oxidation efficiency of gaseous SO_2 by high temperature (Quan et al., 2008). It was suggested that SO_2 was trapped by alkaline aerosol components and oxidize by NO_2 to form sulfate in aqueous media under high RH in winter since air quality models relied on sulfate production mechanisms only requiring photochemical oxidants could not predict that high level sulfate during haze events (Cheng et al., 2016; Wang et al., 2016a). NOR in four seasons were lower than 0.1 and generally consistent, which implied that the secondary conversion of NO_3^- from NO_2 was fairly weak in Kunming compared with secondary SO_4^{2-} formation.

SOR and NOR are consisted of the homogeneous gas-phase transformation via gas-phase chemical processes and heterogeneous reactions. In order to explore the contributions of these two processes to secondary sulfate and nitrate in particle matters, the correlations between RH and SOR (or NOR) were analyzed under different $PM_{2.5}$ levels. As shown in Fig. 5a and Fig. 5b, SOR and NOR showed poor correlations to RH with the increase of $PM_{2.5}$ levels, which illustrated that the heterogeneous reactions perhaps make only a minor contribution to secondary formation of sulfate and nitrate. So higher SOR and NOR values in Kunming city were most likely attributed to the enhancement of gas-phase process. That is different from what reported in Beijing in 2013 that the relatively high SOR values were dominated by heterogeneous reaction under high RH during the haze episode while low NOR values were attributed to gas-phase process (Liu et al., 2016b). Noticing that samples with relatively low $PM_{2.5}$ levels and under high RH conditions distributed in the lower right corner of the graph which were most likely due to precipitation, which showed relatively low SOR and NOR in rainy days.

Pathak et al. (2008) has suggested that the relationship between mole ratio of $[NO_3^-]/[SO_4^{2-}]$ and $[NH_4^+]/[[SO_4^{2-}]$ can be further used to explore the formation pathways of nitrate. Under NH_4^+-rich conditions ($[NH_4^+]/[[SO_4^{2-}] > 1.5$), it has been widely noticed that a linear relationship exists between $[NO_3^-]/[SO_4^{2-}]$ and $[NH_4^+]/[[SO_4^{2-}]$, which was attributed to the homogeneous gas-phase formation of nitrate (HNO_3 (g) + NH_3 (g) = NH_4NO_3 (s,aq)). But under NH_4^+-poor conditions ($[NH_4^+]/[[SO_4^{2-}] < 1.5$), there is no significant correlations can be observed and the high level of nitrate can be associated with the hydrolysis of N_2O_5 in preexisting aerosols (N_2O_5 (aq) + H_2O (aq) = $2NO_3^-$ (aq)+$2H^+$ (aq)).

In this study, the majority of the samples were under the NH^+-rich conditions ($[NH_4^+]/[[SO_4^{2-}] > 1.5$). A good linear correlation was observed between the mole ratio of $[NO_3^-]/[SO_4^{2-}]$ and the $[NH_4^+]/[[SO_4^{2-}]$ ratio under NH_4^+-rich conditions (Fig. 6a), highlighting the

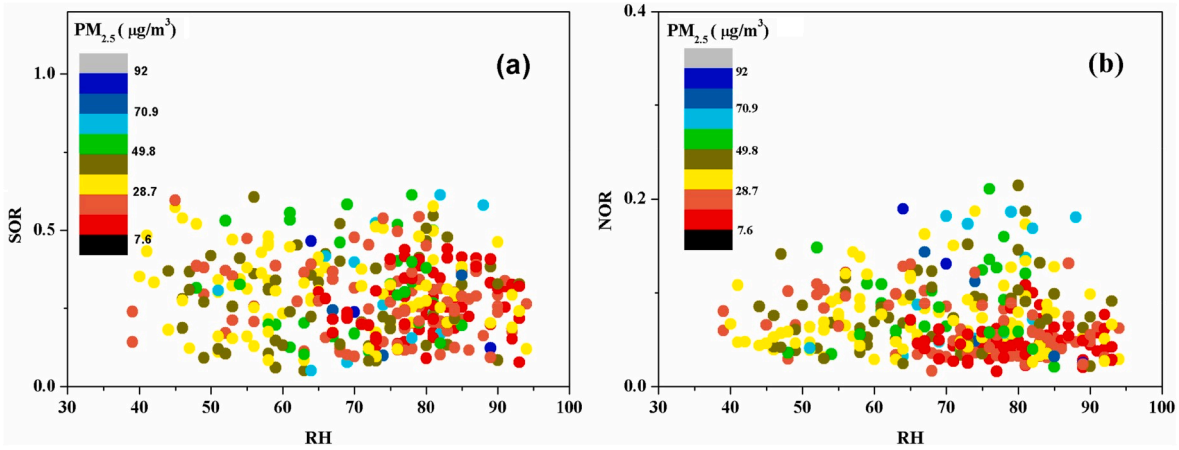

Fig. 5. (a) SOR and (b) NOR plotted against the RH and colored with PM2.5.

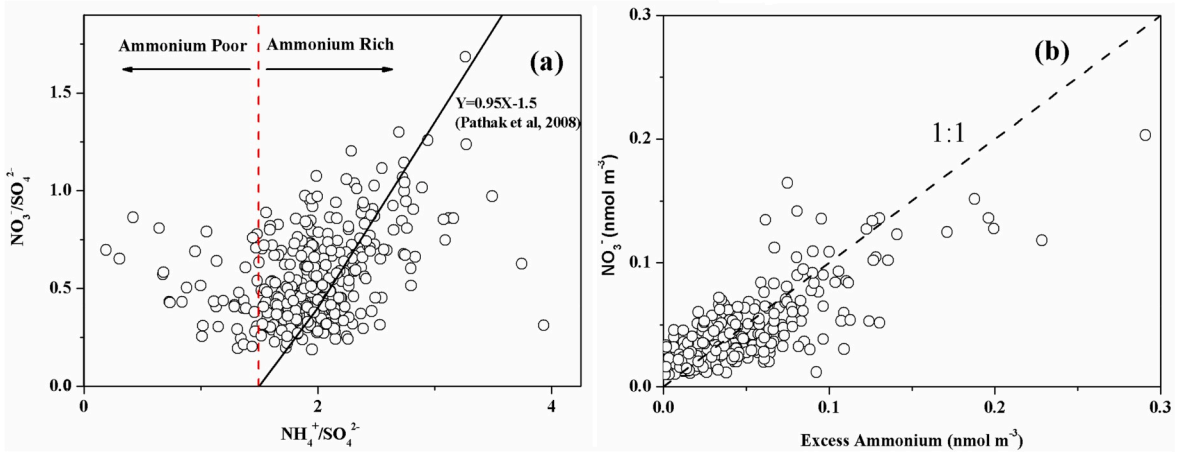

Fig. 6. (a) Nitrate-to-sulfate molar ratio as a function of the ammonium-to-sulfate molar ratio (Fit from (Pathak et al., 2008)) (b) Nitrate concentration as a function of "Excess Ammonium".

homogeneous gas-phase formation of nitrate was evident in aerosol in the NH_3–H^+-SO_4^{2-}-H_2O system. In addition, it could be further confirmed by the good correlation between nitrate concentration and excess ammonium (excess $[NH_4^+] = [NH_4^+] - 1.5[SO_4^{2-}]$) (Fig. 6b). Some processes, like ammonium chloride and sodium nitrate formation, can caused minor influences and made these data slightly deviated from the fit line.

3.2. PMF model

3.2.1. Source apportionment of $PM_{2.5}$ by PMF model

The Positive Matrix Factorization (EPA PMF 5.0) model was used to identify the source categories of $PM_{2.5}$ and their contributions. Five potential sources were identified according to the major WSIIs of aerosol in Kunming. They were (1) dust (including soil dust and construction dust), (2) coal combustion, (3) second inorganic aerosol, (4) biomass burning and (5) sea salt.

The first source was relevant to high loadings of F^- (88.3%), Ca^{2+} (28.5%) and small proportions of Cl^- (19.0%), which were generally derived from dust (soil dust and construction dust), with an annual average contribution of 12.5% to $PM_{2.5}$ (Figs. 7 and 8). Ca^{2+} is a kind of typical crustal element which is mainly generated from weathering process of rocks on the earth surface. The correlation coefficient between F^- and Ca^{2+} was 0.515 (Table 1). Fluorite (CaF_2) is widely used as mineralizer for cement production in construction industry (Chang et al., 2001). In recent years, rapid urbanization of Kunming has accelerated the vigorous development of construction industry. Therefore, construction dust has become one of the non-negligible sources of $PM_{2.5}$ in Kunming.

The second source was assigned to coal combustion, which was identified by Cl^- (67.6%), NO_3^- (35.1%) and SO_4^{2-} (12.1%). Coal combustion is generally utilized in electricity plants, industrial processes, and for winter residential heating mainly in the northern cold regions of China. It contributed 26.0% to $PM_{2.5}$. A key marker for coal combustion including SO_4^{2-} and Cl^- has been reported in other researches (Liu et al., 2016a). Besides coal combustion source (Abdalmogith and Harrison, 2006), Cl^- can also be derived from other sources such as sea salt, biomass burning, and burning of solid waste on small properties especially in developing countries (Vasconcellos et al., 2007).

The third source was characterized by typical compositions of second inorganic aerosol, which contributed 36.3% to total $PM_{2.5}$. The major species of second inorganic aerosol were NO_3^-, SO_4^{2-} and NH_4^+ (53.2%, 68.7% and 78.5% respectively). Many reports have suggested that NO_3^-, SO_4^{2-} and NH_4^+ were mainly derived from gas-particle conversion process. These second inorganic ions in aerosol were formed from the photochemical process or other chemical processes. The contribution of this factor to $PM_{2.5}$ was the highest, and the higher fraction of WSIIs/$PM_{2.5}$ (46–48%) during the sampling period further showed that the highest contribution of this factor to $PM_{2.5}$ was reasonable.

The fourth source was identified as biomass burning, with remarkable K^+ (85.4%), Mg^{2+} (42.8%) and Ca^{2+} (76.1%). It contributed 19.2% to $PM_{2.5}$. K^+ is a major component in the sintering plant stack, and it is

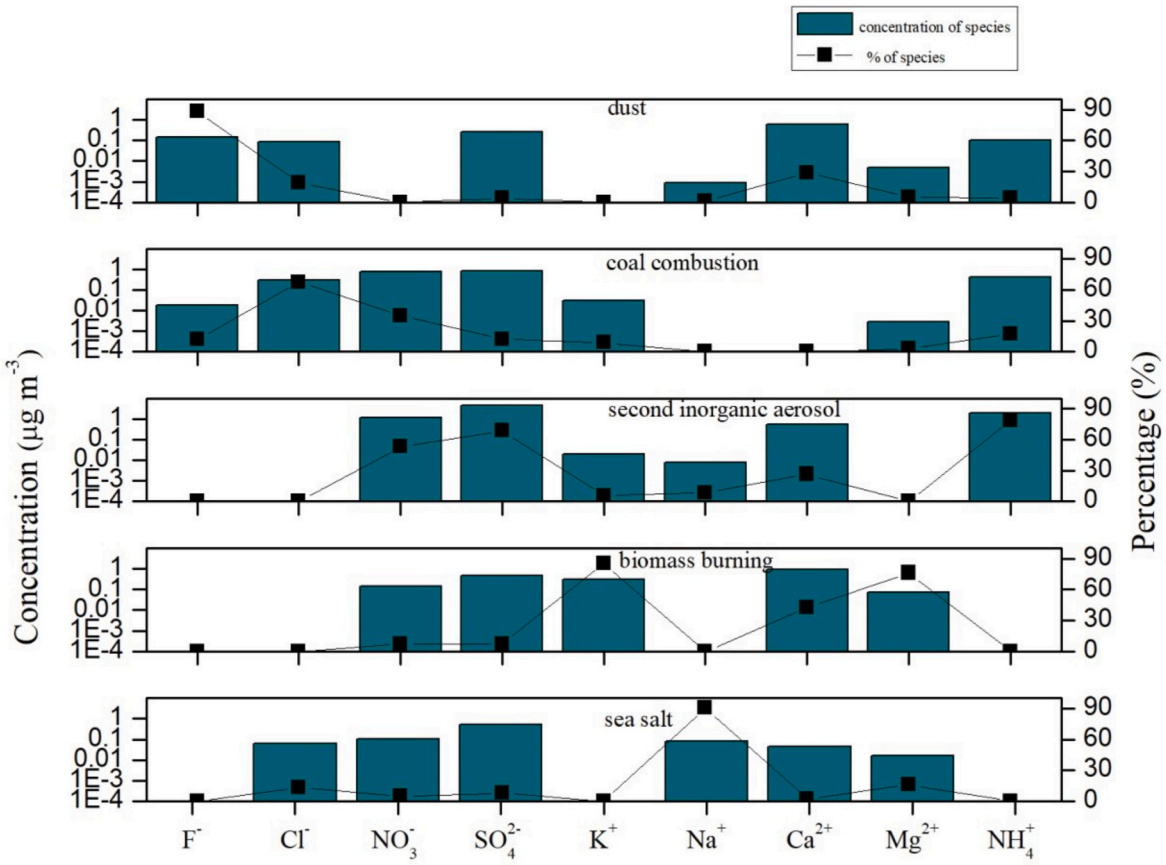

Fig. 7. Profile of five sources identified from EPA PMF 5.0.

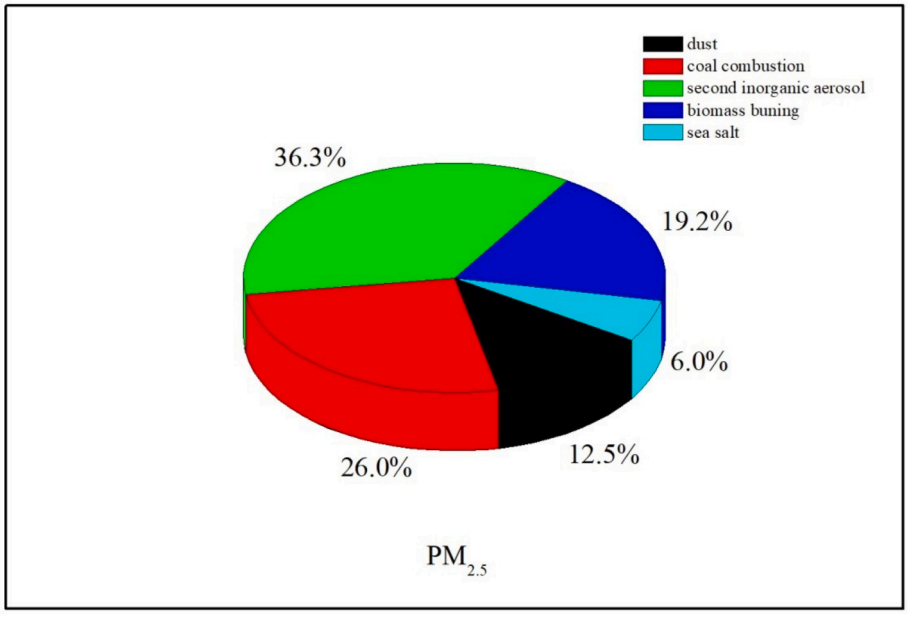

Fig. 8. Average source contributions (in percent) of each identified factor to $PM_{2.5}$ mass in Kunming.

generally a valid indicator of biomass burning (Cheng et al., 2013). Besides, K^+ can be also originated from fossil fuel combustion, biogenic origin and dust (Souza et al., 2014). Mg^{2+} and Ca^{2+}, which are mainly derived from soil dust (Shen et al., 2010) and extremely influenced by temperature and relative humidity, can be released into atmosphere while biomass burning.

The fifth source, with the highest loadings of Na^+, was identified as sea salt (88.8% to Na^+ and 17.7% to Cl^-). The contribution of the fifth source to $PM_{2.5}$ was 6.0% on average. Considering that the Kunming is an inland city, the poor correlations between Cl^- and Na^+ inferred that chlorine depletion could occur by interaction with acidic species and aging during air masses transport (Mkoma et al., 2009).

3.2.2. Annual variations in contributions of different sources

Time series of daily contributions from different sources were exported from PMF 5.0 model. As illustrated in Fig. 9, annual variations in contributions of five sources were reasonably and clearly documented in this study. Higher temperature in warm season (Fig. 2d) could increase the weathering efficiency to create more crustal elements. But the contributions of first factor and the concentrations of F^- and Ca^{2+} in warm season were lower than those in cool season, which were attributed to the frequent precipitations and higher wind speed (Fig. 2a and b). As for coal combustion, the higher contributions mainly appeared in late autumn and winter due to the air pollutants transported from South Asia (especially India) during this season (Section 3). From late autumn to spring, the contributions of biomass burning observably increased rather than in summer. It was ascribed to that air masses from South and Southeast Asia (SEA) took the least proportion in summer (Fig. 10). The contributions of secondary inorganic aerosol were relatively higher in cold season than those in warm season. This seasonal variation pattern was affected by precursor gas and atmosphere condition such as temperature, humidity, insolation and solar radiation. In August, $PM_{2.5}$ has sustained high level (Fig. 3a), which was due to the enhancement of air-particle transformation under strong solar radiation. There was no significant difference in the contributions of sea salt throughout the year. The contribution of sea salt to $PM_{2.5}$ was the lowest, and the slight increase of the concentrations of Na^+ in summer has no obvious effect on the variations of $PM_{2.5}$ in the whole year.

3.3. The backward trajectory analysis

As illustrated in Fig. 10, back-trajectory clustering results of air masses in Kunming were calculated for different seasons. In autumn, trajectory (1), (2), (3), (4) and (5) accounted for 36.2%, 24.2%, 15.4%, 19.8% and 4.4% of total trajectories, respectively. Trajectory (1) began in the Burma. Trajectory (2) was derived from Laos. And trajectory (3) was originated from the border between Vietnam and Guangxi province and passed throng the west Guangxi and the north Vietnam before arriving Kunming. Trajectories (1)–(3) originated from South and Southeast Asia, where biomass burning was the dominant emission source. Trajectories (4) and (5) came from adjacent northeast provinces, Hunan, Guizhou and Sichuan.

In winter, the trajectories (6), (7), (8) and (9) accounted for 46.7%, 38.9%, 8.9% and 5.5% of total trajectories, respectively. Trajectory (6) was originated from northeast India, passed through Bangladesh, Burma before reaching Kunming, which showed the feature of long-distance air transport in winter. Air pollutants might be brought via trajectory (6) from South Asia (especially northeast India), where was considered as a severe haze polluted area during winter. Trajectories (7), (8) and (9) were derived from Burma, local Yunnan and southwest Chinese province, respectively.

In spring, trajectories generally showed the same pattern as those in winter. And the trajectories mainly originated from Bangladesh, northeast India, Burma and south Yunnan province. Trajectories (10), (11), (12) and (13) accounted for 31.5%, 46.8%, 15.2% and 6.5% of the total trajectories, respectively.

In summer, the trajectories (14), (15), (16) and (17) were generated from Burma, Laos, Guangxi and Guizhou province, and the contributions from these four directions are comparable.

It was suggested that the prevailing westerlies showed the variations for the latitude belt between 35°N and 40°N in cold season, and for the belt 45°N ~50°N in warm season (Scherhag, 1948). Prevailing westerlies broke up into two branches when they passed through Pamir Plateau in winter. One branch of the prevailing westerlies traveled along the south rim of the Tibetan Plateau, and the rest one moved along the north rim of the Tibetan Plateau (Yeh, 1957) (Fig. 1). It could be inferred that the trajectories (6) and (10) were both produced by the south branch of the prevailing westerlies and both of them could bring pollutants from South Asia. Trajectory (6) was longer than trajectory (10) while the prevailing westerlies were the strongest in winter and gradually weakened in spring.

Every May to October, air masses from the Indian Ocean to the mainland were brought by the India monsoon to form a rainy season,

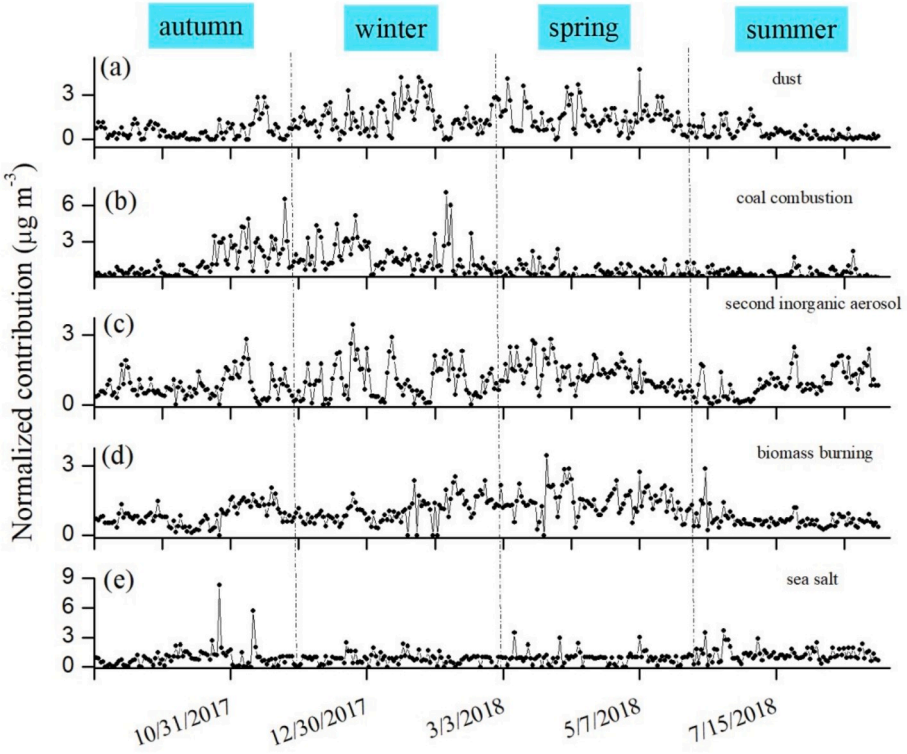

Fig. 9. Time series of daily contributions from each source from PMF model. (x-axis: date-month/day/year).

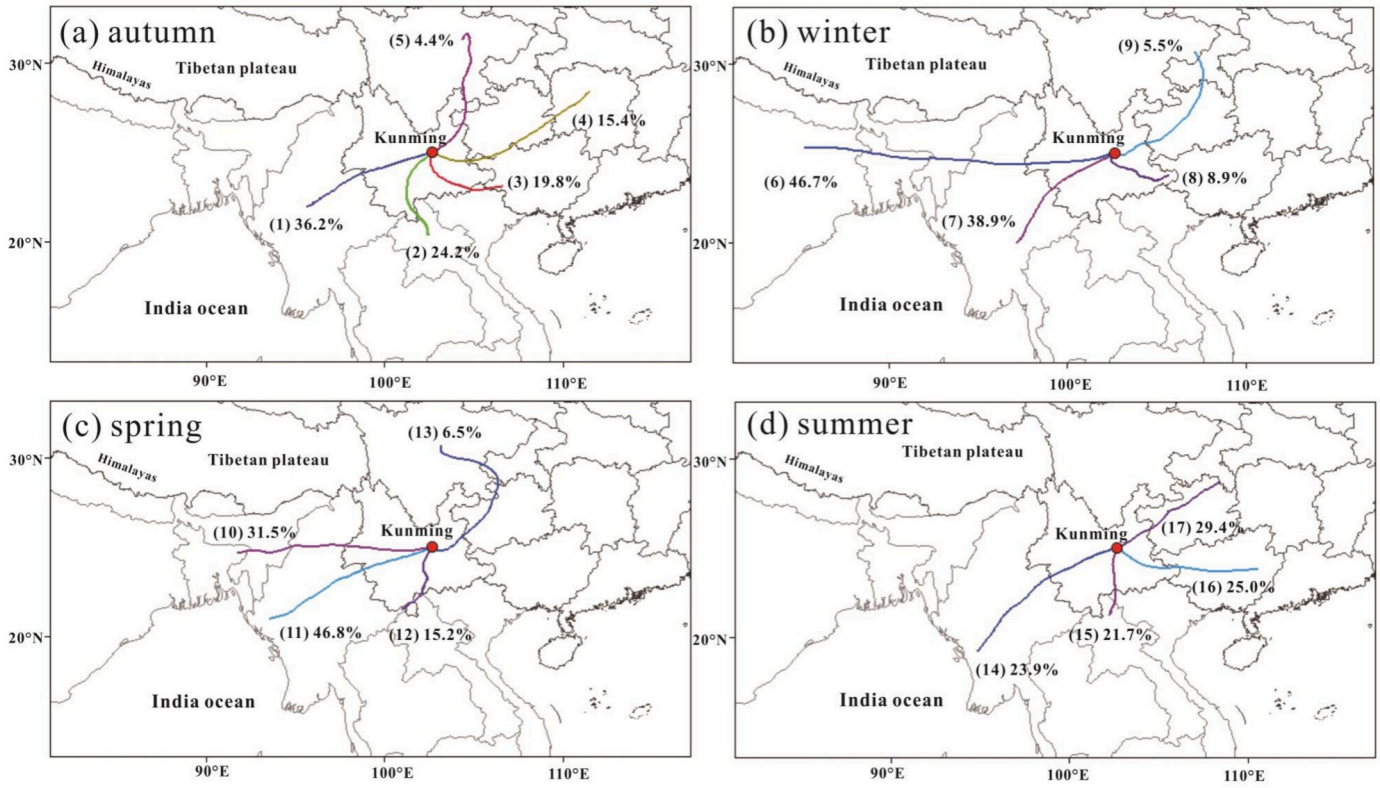

Fig. 10. Back-trajectory clustering results for different seasons at Kunming. (The numbers in bracket are the serial numbers of the trajectories and the proportions of air masses are expressed as a percentage).

while the northeast monsoon formed a dry season from October to May next year (Fig. 1). In other words, driven by summer India monsoon, air pollutants all around South Asia could be gathered to the mountain foot of south Himalayas. Southern India has a long coastline and occasional sea breezes are good for air circulation. The air pollutants gathered in the mountain foot of south Himalayas during cold season reflected the overall polluted characteristics of South Asia. Data from WHO (2016) illustrated that India took up ten seats of the top eleven polluted cities with high $PM_{2.5}$ concentration in the world. Biomass burning during the dry and cold season was regarded as the dominant emission in Southeast Asia and the Indian sub-continent (Duc et al., 2016). But it seemed that people have overlooked the emission from industry to some degree. China and India are the top two consumers of coal in the world. With the rapid development of urbanization and industrialization in India, the massive construction of power plants sharply increased the consumption of coal. From 2007 to 2016, SO_2 emissions from coal combustion have declined by 75% in China owing to the application of desulfurization process. However, the emissions of SO_2 have increased by 50% in India. India has surpassed China to be the largest emitter of anthropogenic SO_2 since 2016 (Li et al., 2017a). The neglect of pollutant emission control and lack of vigorous control over coal desulfurization have made India one of the most polluted areas in the world.

It could be inferred from Figs. 9 and 10, air pollutants derived from South Asia (especially India) were most likely to be brought to Kunming by air masses from trajectory (6), and this was coincident with the significant increase in factor contributions of coal combustion in winter (Fig. 9b). Near the end of the cool and dry northeast monsoon before the onset of the wet southwest monsoon and during the peak of the annual agricultural biomass burning in SEA in March, a circulation loop of air flow brought air pollutants from biomass burning in SEA to southern China (Duc et al., 2016). In spring, it's difficult for air masses from trajectory (10) to bring pollutants emitted from coal combustion in India to Kunming when prevailing westerlies gradually weakened. And the sources of $PM_{2.5}$ in Kunming were mainly affected by biomass burning from South Asia and Southeast Asia this season. This corresponded to the sharp decrease in the factor contributions of coal combustion and the increase in factor contributions of biomass combustion simulated in our PMF in spring (Fig. 9d). Generally, the persistent severe pollution in India will have direct and profound impact on the air quality in the urban area of Kunming.

4. Conclusion

The water-soluble inorganic ions of ambient $PM_{2.5}$ from September 2017 to August 2018 were investigated in Kunming to better understand the chemical characteristics, source categories and potential origin of pollutants. The annual average concentration of $PM_{2.5}$ was 33.59 ± 15.71 μg m^{-3}. Except for Na^+, the other major WSIIs showed the same seasonal variation patterns as $PM_{2.5}$, with higher concentrations in the cool season than in the warm season. It could be inferred from the mass ratio of NO_3^-/SO_4^{2-} that there were fewer stationary sources and fewer mobile sources in Kunming compared to other cities. The variations of SOR illustrated that secondary formation of sulfate occurred every season and was more efficient in spring. The values of NOR indicated fairly weak secondary nitrate formation in four seasons.

Major sources of $PM_{2.5}$ identified from positive matrix factorization (PMF) model included secondary aerosol, coal combustion, biomass burning, dust and sea salt, which contributed 36.3%, 26.0%, 19.2%, 12.5% and 6.0% to $PM_{2.5}$, respectively. The contributions of sea salt kept unchanged for the whole year. Source ratio of coal combustion just increased in late autumn and winter, and the contributions of other sources were higher in cold season than those in warm season. Generally, coal combustion played a leading role in the source contribution of $PM_{2.5}$ in winter while biomass combustion was dominant in spring.

Seasonal back-trajectory clustering results were computed to track the origin of air masses. In winter, air masses from South Asia (especially

India) contained pollutants mainly derived from coal combustion could be brought to Kunming by prevailing westerlies. In spring, the sources of $PM_{2.5}$ in Kunming were mainly affected by biomass burning from South Asia and Southeast Asia when prevailing westerlies gradually weakened.

Declaration of competing interest

The authors declare that they have no known competing financial interests or personal relationships that could have appeared to influence the work reported in this paper.

CRediT authorship contribution statement

Yunhong Zhou: Methodology, Data curation, Writing - original draft. **Huayun Xiao:** Conceptualization, Methodology, Supervision, Writing - review & editing. **Hui Guan:** Methodology, Supervision, Writing - review & editing. **Nengjian Zheng:** Data curation, Investigation. **Zhongyi Zhang:** Data curation, Investigation. **Jing Tian:** Investigation, Visualization. **Linglu Qu:** Investigation, Visualization. **Jingjing Zhao:** Investigation, Visualization. **Hongwei Xiao:** Visualization.

Acknowledgments

This study was kindly supported by the National Natural Science Foundation of China through grant numbers 41425014, 41603017 and 41863001, the National Key Research and Development Program of China through grant number 2016YFA0601000.

Appendix A. Supplementary data

Supplementary data to this article can be found online at https://doi.org/10.1016/j.atmosenv.2020.117704.

References

Abdalmogith, S.S., Harrison, R.M., 2006. An analysis of spatial and temporal properties of daily sulfate, nitrate and chloride concentrations at UK urban and rural sites. J. Environ. Monit. 8, 691–699.
Almeida, S.M., Lage, J., Fernandez, B., Garcia, S., Reis, M.A., Chaves, P.C., 2015. Chemical characterization of atmospheric particles and source apportionment in the vicinity of a steelmaking industry. Sci. Total Environ. 521–522, 411–420.
Cao, J.J., Shen, Z.X., Chow, J.C., Qi, G.W., Watson, J.G., 2009. Seasonal variations and sources of mass and chemical composition for PM_{10} aerosol in Hangzhou, China. Particuology 7, 161–168.
Chang, J., Cheng, X., Liu, F.T., Lu, L.C., Teng, B., 2001. Influence of fluorite on the Ba-bearing sulphoaluminate cement. Cement Concr. Res. 31, 213–216.
Cheng, Y., Engling, G., He, K.B., Duan, F.K., Ma, Y.L., Du, Z.Y., et al., 2013. Biomass burning contribution to Beijing aerosol. Atmos. Chem. Phys. 13, 7765–7781.
Cheng, Y.F., Zheng, G.J., Wei, C., Mu, Q., Zheng, B., Wang, Z.B., et al., 2016. Reactive nitrogen chemistry in aerosol water as a source of sulfate during haze events in China. Sci. Adv. 2, e1601530.
Chin, M., Kahn, R.A., Remer, L.A., Yu, H.B., Rind, D., Feingold, G., et al., 2009. Atmospheric aerosol properties and climate impacts. Environ. Pol. Collect. 28, 302–307.
Chow, J.C., Watson, J.G., Mauderly, J.L., Costa, D.L., Wyzga, R.E., Vedal, S., et al., 2006. Health effects of fine particulate air pollution: lines that connect. J. Air Waste Manag. Assoc. 56, 1368–1380.
Dockery, D.W., Pope, C.A., Xu, X.P., Spengler, J.D., Ware, J.H., Fay, M.E., et al., 1993. An association between air-pollution and mortality in 6 united-states cities. N. Engl. J. Med. 329, 1753–1759.
Duc, H.N., Bang, Q., Quang, N.X., 2016. Modelling and prediction of air pollutant transport during the 2014 biomass burning and forest fires in peninsular Southeast Asia. Environ. Monit. Assess. 188, 106.
Engelbrecht, J.P., Kavouras, I.G., Shafer, D.S., Campbell, D., Campbell, S., McCurdy, G., et al., 2015. Chemical variability of PM_{10} and $PM_{2.5}$ in southwestern rural Nevada, USA. Water Air Soil Pollut. 226, 217.
Gerasopoulos, E., Koulouri, E., Kalivitis, N., Kouvarakis, G., Saarikoski, S., Makela, T., et al., 2007. Size-segregated mass distributions of aerosols over Eastern Mediterranean: seasonal variability and comparison with AERONET columnar size-distributions. Atmos. Chem. Phys. 7, 2551–2561.
Heal, M.R., Hibbs, L.R., Agius, R.M., Beverland, L.J., 2005. Total and water-soluble trace metal content of urban background PM_{10}, $PM_{2.5}$ and black smoke in Edinburgh, UK. Atmos. Environ. 39, 1417–1430.
Hu, M., He, L.Y., Zhang, Y.H., Wang, M., Kim, Y.P., Moon, K.C., 2002. Seasonal variation of ionic species in fine particles at Qingdao, China. Atmos. Environ. 36, 5853–5859.
Lawrence, M.G., Lelieveld, J., 2010. Atmospheric pollutant outflow from southern Asia: a review. Atmos. Chem. Phys. 10, 11017–11096.
Li, C., McLinden, C., Fioletov, V., Krotkov, N., Carn, S., Joiner, J., et al., 2017a. India is overtaking China as the world's largest emitter of anthropogenic sulfur dioxide. Sci. Rep. 7, 14304.
Li, Z.Q., Guo, J.P., Ding, A.J., Liao, H., Liu, J.J., Sun, Y.L., et al., 2017b. Aerosol and boundary-layer interactions and impact on air quality. Nat. Sci. Rev. 4, 810–833.
Liu, B.S., Song, N., Dai, Q.L., Mei, R.B., Sui, B.H., Bi, X.H., et al., 2016a. Chemical composition and source apportionment of ambient $PM_{2.5}$ during the non-heating period in Taian, China. Atmos. Res. 170, 23–33.
Liu, B.S., Wu, J.H., Zhang, J.Y., Wang, L., Yang, J.M., Liang, D.N., et al., 2017. Characterization and source apportionment of $PM_{2.5}$ based on error estimation from EPA PMF 5.0 model at a medium city in China. Environ. Pollut. 222, 10–22.
Liu, Z.R., Gao, W.K., Yu, Y.C., Hu, B., Xin, J.Y., Sun, Y., et al., 2018. Characteristics of $PM_{2.5}$ mass concentrations and chemical species in urban and background areas of China: emerging results from the CARE-China network. Atmos. Chem. Phys. 18, 8849–8871.
Liu, Z.R., Hu, B., Zhang, J.K., Yu, Y.C., Wang, Y.S., 2016b. Characteristics of aerosol size distributions and chemical compositions during wintertime pollution episodes in Beijing. Atmos. Res. 168, 1–12.
Luo, L., Wu, Y.F., Xiao, H.Y., Zhang, R.J., Lin, H., Zhang, X.L., et al., 2019. Origins of aerosol nitrate in Beijing during late winter through spring. Sci. Total Environ. 653, 776–782.
Mkoma, S.L., Maenhaut, W., Chi, X.G., Wang, W., Raes, N., 2009. Characterisation of PM_{10} atmospheric aerosols for the wet season 2005 at two sites in East Africa. Atmos. Environ. 43, 631–639.
Ohta, S., Okita, T., 1990. A chemical characterization of atmospheric aerosol in Sapporo. Atmos. Environ. Gen. Top 24, 815–822.
Ou, J.Y., Hanson, H.A., Ramsay, J.M., Leiser, C.L., Zhang, Y., VanDerslice, J.A., et al., 2019. Fine particulate matter and respiratory healthcare encounters among survivors of childhood cancers. Int. J. Environ. Res. Publ. Health 16, 1081.
Paatero, P., 1997. Least squares formulation of robust non-negative factor analysis. Chemometr. Intell. Lab. Syst. 37, 23–35.
Paatero, P., Tapper, U., 1994. Positive matrix factorization - a nonnegative factor model with optimal utilization of error-estimates of data values. Environmetrics 5, 111–126.
Pant, P., Harrison, R.M., 2012. Critical review of receptor modelling for particulate matter: a case study of India. Atmos. Environ. 49, 1–12.
Pathak, R.K., Wu, W.S., Wang, T., 2008. Summertime $PM_{2.5}$ ionic species in four major cities of China: nitrate formation in an ammonia-deficient atmosphere. Atmos. Chem. Phys. Discuss. 8.
Polissar, A.V., Hopke, P.K., Paatero, P., Malm, W.C., Sisler, J.F., 1998. Atmospheric aerosol over Alaska: 2. Elemental composition and sources. J. Geophys. Res.: Atmospheres 103, 19045–19057.
Pope, C.A.I., Majid, E., Douglas W, D., 2009. Fine-particulate air pollution and life expectancy in the United States. N. Engl. J. Med. 360, 376.
Pope, C.A.I., Turner, M.C., Burnett, R.T., Jerrett, M., Gapstur, S.M., Diver, W.R., et al., 2015. Relationships between fine particulate air pollution, cardiometabolic disorders, and cardiovascular mortality. Circ. Res. 116, 108–115.
Qiao, X., Ying, Q., Li, X.H., Zhang, H.L., Hu, J.L., Tang, Y., et al., 2018. Source apportionment of $PM_{2.5}$ for 25 Chinese provincial capitals and municipalities using a source-oriented Community Multiscale Air Quality model. Sci. Total Environ. 612, 462–471.
Qin, N.X., Chen, X., Fu, G.B., Zhai, J.Q., Xue, X.W., 2010. Precipitation and temperature trends for the Southwest China: 1960-2007. Hydrol. Process. 24, 3733–3744.
Quan, J.N., Zhang, X.S., Zhang, Q., Guo, J.H., Vogt, R.D., 2008. Importance of sulfate emission to sulfur deposition at urban and rural sites in China. Atmos. Res. 89, 283–288.
Ramgolam, K., Favez, O., Cachier, H., Gaudichet, A., Marano, F., Martinon, L., et al., 2009. Size-partitioning of an urban aerosol to identify particle determinants involved in the proinflammatory response induced in airway epithelial cells. Part. Fibre Toxicol. 6, 10.
Scherhag, R., 1948. Neue Methoden der Wetteranalyse und Wetterprognose. Springer-Verlag, p. 424.
Sharma, S.K., Mandal, T.K., Jain, S., Saraswati Sharma, A., Saxena, M., 2016. Source apportionment of $PM_{2.5}$ in Delhi, India using PMF model. Bull. Environ. Contam. Toxicol. 97, 286–293.
Shen, Z.X., Cao, J.J., Arimoto, R., Han, Y.M., Zhu, C.S., Tian, J., et al., 2010. Chemical characteristics of fine particles (PM_1) from Xi'an, China. Aerosol. Sci. Technol. 44, 461–472.
Shi, J.W., Ding, X., Zhou, Y., You, R., Huang, L., Hao, J.M., et al., 2016. Characteristics of chemical components in $PM_{2.5}$ at a plateau city, South-west China. Front. Environ. Sci. Eng. 10.
Souza, D.Z., Vasconcellos, P.C., Lee, H., Aurela, M., Saarnio, K., Teinilae, K., et al., 2014. Composition of $PM_{2.5}$ and PM_{10} collected at urban sites in Brazil. Aerosol Air Qual. Res. 14, 168–176.
Sun, Y.L., Zhuang, G.S., Tang, A.H., Wang, Y., An, Z.S., 2006. Chemical characteristics of $PM_{2.5}$ and PM_{10} in haze-fog episodes in Beijing. Environ. Sci. Technol. 40, 3148–3155.
Tan, J.H., Duan, J.C., Chen, D.H., Wang, X.H., Guo, S.J., Bi, X.H., et al., 2009. Chemical characteristics of haze during summer and winter in Guangzhou. Atmos. Res. 94, 238–245.
Tang, I.N., 1996. Chemical and size effects of hygroscopic aerosols on light scattering coefficients. J. Geophys. Res. Atmosphere 101, 19245–19250.

Tao, J., Zhang, L.M., Engling, G., Zhang, R.J., Yang, Y.H., Cao, J.J., et al., 2013. Chemical composition of $PM_{2.5}$ in an urban environment in Chengdu, China: importance of springtime dust storms and biomass burning. Atmos. Res. 122, 270–283.

Vasconcellos, P.C., Balasubramanian, R., Bruns, R.E., Sanchez-Ccoyllo, O., Andrade, M. F., Flues, M., 2007. Water-soluble ions and trace metals in airborne particles over urban areas of the state of sauo paulo, Brazil: influences of local sources and long range transport. Water Air Soil Pollut. 186, 63–73.

Wang, G.H., Zhang, R.Y., Gomez, M.E., Yang, L.X., Zamora, M.L., Hu, M., et al., 2016a. Persistent sulfate formation from London Fog to Chinese haze. Proc. Natl. Acad. Sci. U.S.A. 113, 13630–13635.

Wang, P., Cao, J.J., Shen, Z.X., Han, Y.M., Lee, S.C., Huang, Y., et al., 2015. Spatial and seasonal variations of $PM_{2.5}$ mass and species during 2010 in Xi'an, China. Sci. Total Environ. 508, 477–487.

Wang, Y., Zhuang, G., Zhang, X., Huang, K., Xu, C., Tang, A., et al., 2006. The ion chemistry, seasonal cycle, and sources of PM2.5 and TSP aerosol in Shanghai. Atmos. Environ. 40, 2935–2952.

Wang, Y., Zhuang, G.S., Tang, A.H., Yuan, H., Sun, Y.L., Chen, S.A., et al., 2005. The ion chemistry and the source of $PM_{2.5}$ aerosol in Beijing. Atmos. Environ. 39, 3771–3784.

Wang, Y.N., Jia, C.H., Tao, J., Zhang, L.M., Liang, X.X., Ma, J.M., et al., 2016b. Chemical characterization and source apportionment of $PM_{2.5}$ in a semi-arid and petrochemical-industrialized city, Northwest China. Sci. Total Environ. 573, 1031–1040.

Word Health Organization (WHO), 2016. https://www.who.int/gho/phe/outdoor_air_pollution/outdoor_air_pollution_mapPM25_WHOborders_notext.pdf.

Word Health Organization (WHO), 2018. 9 Out of 10 People Worldwide Breathe Polluted Air, but More Countries Are Taking Action. https://www.who.int/news-room/detail/02-05-2018-9-out-of-10-people-worldwide-breathe-polluted-air-but-more-countries-are-taking-action.

Xiao, H.W., Xiao, H.Y., Luo, L., Shen, C.Y., Long, A.M., Chen, L., et al., 2017. Atmospheric aerosol compositions over the South China Sea: temporal variability and source apportionment. Atmos. Chem. Phys. 17, 3199–3214.

Xiao, H.Y., Liu, C.Q., 2004. Chemical characteristics of water-soluble components in TSP over Guiyang, SW China, 2003. Atmos. Environ. 38, 6297–6306.

Xu, L., Batterman, S., Chen, F., Li, J., Zhong, X., Feng, Y., et al., 2017. Spatiotemporal characteristics of $PM_{2.5}$ and PM_{10} at urban and corresponding background sites in 23 cities in China. Sci. Total Environ. 599–600, 2074–2084.

Xu, L.L., Chen, X.Q., Chen, J.S., Zhang, F.W., He, C., Zhao, J.P., et al., 2012. Seasonal variations and chemical compositions of $PM_{2.5}$ aerosol in the urban area of Fuzhou, China. Atmos. Res. 104, 264–272.

Yao, X.H., Chan, C.K., Fang, M., Cadle, S., Chan, T., Mulawa, P., et al., 2002. The water-soluble ionic composition of $PM_{2.5}$ in Shanghai and Beijing, China. Atmos. Environ. 36, 4223–4234.

Yao, X.H., Fang, M., Chan, C.K., 2003. The size dependence of chloride depletion in fine and coarse sea-salt particles. Atmos. Environ. 37, 743–751.

Ye, B.M., Ji, X.L., Yang, H.Z., Yao, X.H., Chan, C.K., Cadle, S.H., et al., 2003. Concentration and chemical composition of $PM_{2.5}$ in Shanghai for a 1-year period. Atmos. Environ. 37, 499–510.

Yeh, T.C., 1957. The wind structure and heat balance in the lower troposphere over Tibetan plateau and its surrounding, 28. Institute of Meterorology and Geophysics, pp. 108–121.

Yin, D.Y., Zhao, S.P., Qu, J.J., 2016. Spatial and seasonal variations of gaseous and particulate matter pollutants in 31 provincial capital cities, China. Air Qual. Atmosphere Health 10, 359–370.

Yuan, M., Huang, Y.P., Shen, H.F., Li, T.W., 2018. Effects of urban form on haze pollution in China: spatial regression analysis based on $PM_{2.5}$ remote sensing data. Appl. Geogr. 98, 215–223.

Zhang, F., Cheng, H.R., Wang, Z.W., Lv, X.P., Zhu, Z.M., Zhang, G., et al., 2014. Fine particles ($PM_{2.5}$) at a CAWNET background site in Central China: chemical compositions, seasonal variations and regional pollution events. Atmos. Environ. 86, 193–202.

Zhang, Q.H., Zhang, J.P., Xue, H.W., 2010. The challenge of improving visibility in Beijing. Atmos. Chem. Phys. 10, 7821–7827.

Zhao, P.S., Dong, F., He, D., Zhao, X.J., Zhang, X.L., Zhang, W.Z., et al., 2013. Characteristics of concentrations and chemical compositions for $PM_{2.5}$ in the region of Beijing, Tianjin, and Hebei, China. Atmos. Chem. Phys. 13, 4631–4644.